Microalgal biofilm behavior under light/dark cycles

Yan Gao, J. Ignacio Fierro U, Patrick Perré, Filipa Lopes, Olivier Bernard

Microalgal biofilm behavior under light/dark cycles

Yan Gao * **J. Ignacio Fierro U.** *** **Patrick Perré** **
Filipa Lopes * **Olivier Bernard** ***

* *Université Paris-Saclay, CentraleSupélec, LGPM, Gif-sur-Yvette, 91190, France*
** *Université Paris-Saclay, CentraleSupélec, LGPM, CEBB, Pomacle, 51110, France*
*** *Biocore, Inria Sophia Antipolis Méditerranée, Université Nice Côte d'Azur, 06902 France (e-mail: olivier.bernard@inria.fr)*

Abstract: Biofilm-based systems have attracted more attention recently as an alternative to the standard suspended-cells process for microalgae cultivation. It has also been shown that cells can be protected from photoinhibition under intense sunlight when submitted to alternately light and dark cycles. However, the biological response to light variation is not well understood. Therefore, in this work, a mechanistic model is developed based on Han's model to describe photosynthesis and respiration dynamics that cover different cycle times and a wide range of light fractions (Light/Dark fractions). Keeping the same average light intensity, increasing the light frequency enhances growth thanks to reduced photoinhibition. Increasing light fraction improves the growth rate as both the peak light intensity and the dark period decrease. Respiration variation in intermittent light regimes is for the first time considered in this model, giving a better explanation of biofilm growth experimental data. Understanding the model response will guide strategies for growth enhancement, and further optimize biofilm reactor design and operation and eventually benefit biomass productivity.

Keywords: Microalgae, biofilm growth, L/D cycles, modeling.

1. INTRODUCTION

Microalgae are regarded as one of the most promising resources for producing food, animal feed, pharmaceuticals, and long-term biofuels (Mata et al., 2010; Bhattacharya and Goswami, 2020). They are mainly cultivated in suspension-based systems (Costa et al., 2019), with an actual yield significantly lower than the theoretical ones. The high economical cost of cultivation is due, in a large fraction, to harvesting (Milledge and Heaven, 2013). This has motivated a recent interest in biofilm-based microalgae technology (Mantzorou and Ververidis, 2019). Unlike planktonic cells suspended in the medium, microalgae biofilms are thin slimy layers of microalgae that attach and grow on solid surfaces (Mantzorou and Ververidis, 2019). One of the most interesting advantage of biofilm-based technologies is that harvesting is easy to proceed just by scraping off the biofilm from the surface.

⋆ We thank the financial support of China Scholarship Council and ANR PhotoBiofilm Explorer (Project-ANR-20-CE43-0008) /LaSIPS Greenbelt. We thank also the Département de la Marne, Grand Reims, Région Grand Est and the European Union along with the European Regional Development Fund (ERDF Champagne Ardenne 2014-2020) for their financial support of the Chair of Biotechnology of CentraleSupélec. This work benefited from the ITN Digitalgaesation project funded by the European Union's Horizon 2020 research, and innovation program under the Marie Skłodowska-Curie grant agreement No. 955520.

Various biofilm reactors with different configurations were developed, as summarized by (Wang et al., 2017). Biofilm reactor design and operation are related to the light regimes received by the attached microalgal cells. Especially, in revolving biofilm systems partially submerged in liquid, cells are submitted to dark periods which may mitigate photoinhibition caused by the constant exposure to intense sunlight. Here, we focus on the process by which the cells in the biofilm grow in periodic light-dark cycles. The light fraction, which is an operating factor, refers to the ratio between the time of exposure to sunlight to the cycle time (T) (Gross et al., 2015). The growth rate (μ) of the biofilm under periodic light regimes depends on the cycle time (T), the light fraction (or duty cycle, ε) and the light intensity (I_{peak}) during the illumination period. The impact of fluctuating light on growth has been mainly investigated in planktonic cultures. It was demonstrated that photoinhibition can be reduced by decreasing the cycle time, reaching a flashing regime tending to continuous light of averaged light intensity, which is called *full light integration* in literature (Sforza et al., 2012). All the photons are then used when the flash time is short enough (e.g., in milliseconds scale, (Vejrazka, 2012)). This phenomenon corresponds to when photosynthesis rate enhancement is maximal while inhibition is minimal so that the average growth rate is $\mu_S(I_{peak} \cdot \varepsilon)$, where μ_S is the growth rate at steady state. Inappropriate L/D cycles, induce growth penalty (Graham et al., 2017). By comparison, the so-called *no light integration* describes that photoinhibition

is maximal, with no improvement of photosynthesis rate, due to long light/dark periods (so that the average growth rate is $\mu_S(I_{peak}) \cdot \varepsilon$) (Graham et al., 2017).

By contrast, only a few studies have focused on biofilms subjected to fluctuating light regimes (Toninelli et al., 2016; Martín-Girela et al., 2017). For instance, (Toninelli et al., 2016) studied biofilms of *Scenedesmus dimorphus* exposed to fluctuating light with T ranging from 0.2 s to 24 h and with ε of 0.33 and 0.5. They observed an increase in the photoefficiency when decreasing T. In biofilms, unlike planktonic cultures in high density reactors, the light regime is entirely controlled by the reactor design and operation. It is therefore identical for all cells which experience the same T (related to rotation speed) and the same ε (related to the reactor design). Only the light intensity changes according to biofilm depth, due to the light attenuation within the biofilm(Huang et al., 2016). The biological response of biofilm cells to intermittent light is not fully understood yet (Toninelli et al., 2016). A detailed insight into photosynthesis dynamics response and quantitative and predictive models are still required (Vejrazka, 2012). In addition, the models presented in the literature have ignored respiration variation in intermittent light regimes, biasing the estimations of net growth and productivity (Beardall et al., 1994).

Therefore, to simulate biofilm growth and understand the effect of intermittent light regimes, we propose here a model considering the biofilm thickness and including respiration variation in light/dark periods. We compute the average growth rate in periodic light regimes. The model calibration and validation were guided by experiments performed with *Chlorella vulgaris* biofilms subjected to four continuous light regimes and six light/dark regimes. Finally, the model's ability to predict various light regime is discussed.

2. MODEL DEVELOPMENT

This model is developed based on the mechanistic model of (Han, 2002) to integrate the effect of photoinhibition on photosynthesis. It is based on the assumption that the reaction centers can be categorized in three states (Megard et al., 1984): open and ready for catching photons A, closed while processing photons B, or inhibited when some key proteins (D1) get damaged due to an excess of energy resulting from too many harvested photons C. The states A, B and C represent the proportion of the three states of photosynthetic units in each of these states. Therefore, it follows that:

$$A + B + C = 1 \tag{1}$$

The dynamics of the three states of the model is given by:

$$\begin{cases} \dot{A} = -\sigma I A + \dfrac{B}{\tau}, \\ \dot{B} = \sigma I A - \dfrac{B}{\tau} + k_r C - k_d \sigma I B, \\ \dot{C} = -k_r C + k_d \sigma I B. \end{cases} \tag{2}$$

Here σ (μmol$^{-1}\cdot$m^2) is the cross-section of PSII; τ (s) represents the turnover time of the electron transfer chain. k_d (dimensionless) is the damage rate and k_r (s^{-1}) is the repair rate. The system (2) can be reduced using (1) into a two-dimensional system:

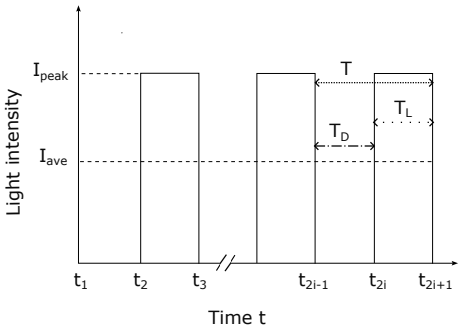

Fig. 1. Graphic description of the light pattern.

$$\begin{cases} \dot{A} = -\left(\sigma I + \dfrac{1}{\tau}\right) A + \dfrac{1-C}{\tau}, & \text{(3a)} \\ \dot{C} = -\left(k_r + k_d \sigma I\right) C + k_d \sigma I (1 - A). & \text{(3b)} \end{cases}$$

The gross growth rate, which is the rate of carbon fixation from the Calvin cycle, can then be written as:

$$\mu = k \sigma I A. \tag{4}$$

Where k ($s \cdot s^{-}1$) is a scaling factor, linking the rate of photons capture to the microalgae growth rate.

In this paper, we consider piece-wise constant light/dark cycles with period T. The biofilm is exposed to a light intensity I_{peak} for a time of $T_L = \varepsilon T$ and then the biofilm remains in darkness for a time $T_D = (1-\varepsilon)T$. We denote by t_{2i-1} the moment when dark period starts; by t_{2i} the moment when light period starts; and by t_{2i+1} the moment when a cycle finishes. This light pattern is presented in Fig. 1.

2.1 Light/dark periods shorter than seconds

When the light changes rapidly, the dynamics of C is too slow to change, then we reduce the dynamics (3a) and (3b) into one equation assuming that C remains constant (Hartmann et al., 2014) and we denote this value as $\bar{C}$. The dynamic of state A during the light phase is then deduced from Equation (3a) as a function of I:

$$\begin{aligned} A(t) = \frac{1-\bar{C}}{\tau\sigma I + 1}\left(1 - e^{-\left(\sigma I + \frac{1}{\tau}\right)(t - t_{2i})}\right) \\ + A(t_{2i}) e^{-\left(\sigma I + \frac{1}{\tau}\right)(t - t_{2i})}, \end{aligned} \tag{5}$$

where

$$\begin{aligned} A(t_{2i}) = (1-\bar{C})g,\ g = \frac{(1 - x + \frac{1-y}{\sigma I \tau + 1} x)}{1 - xy}, \\ x = e^{-\frac{T(1-\varepsilon)}{\tau}},\ y = e^{-(\sigma I + \frac{1}{\tau})T\varepsilon}. \end{aligned} \tag{6}$$

The average value of A in the light phase ($t \in [t_{2i}, t_{2i+1}]$) (light period integrated, noted as $\bar{A}_L$) is expressed by:

$$\bar{A}_L = \frac{1}{T\varepsilon} \int_{t_{2i}}^{t_{2i+1}} A(t)\, dt = (1-\bar{C})h, \tag{7}$$

where

$$h = \frac{1}{\sigma I \tau + 1} + \left(\frac{1}{\sigma I \tau + 1} - g\right) \cdot \frac{1}{T\varepsilon\left(\sigma I + \frac{1}{\tau}\right)} \cdot (y - 1),$$

To get $\bar{C}$, the asymptotic value of C, we do a cycle time integration at two sides of Equation (3b):

$$\int_{t_{2i-1}}^{t_{2i+1}} \dot{C}dt = \int_{t_{2i-1}}^{t_{2i+1}} -k_r C + k_d\sigma I - k_d\sigma IA - k_d\sigma IC\, dt, \tag{8}$$

Since in periodic regime $C(t_{2i-1}) = C(t_{2i+1})$, we get:

$$\begin{aligned} 0 &= -k_r CT + k_d\sigma IT\varepsilon + k_d\sigma ICT\varepsilon \\ &\quad - \int_{t_{2i}}^{t_{2i+1}} k_d\sigma IA(t)\, dt, \\ \bar{C} &= \frac{k_d\sigma I - k_d\sigma Ih}{\frac{k_r}{\varepsilon} - k_d\sigma Ih + k_d\sigma I}. \end{aligned} \tag{9}$$

The average gross growth rate (light period integrated, noted as $\bar{\mu}_L$) in light phase ($t \in [t_{2i}, t_{2i+1}]$) is then:

$$\bar{\mu}_L(I) = \frac{1}{T\varepsilon} \cdot \int_{t_{2i}}^{t_{2i+1}} k\sigma IA(t)\, dt = k\sigma I\bar{A}_L. \tag{10}$$

2.2 Light/dark periods longer than seconds

As studied by (Bara et al., 2019), for light/dark periods a range of order longer than the time constant characterizing its dynamics, A reaches its pseudo steady state quickly in the light phase and then in the dark phase. State A very rapidly converges to the following function of C:

$$A = \frac{1 - C}{1 + \tau\sigma I}. \tag{11}$$

Then the dynamics of C in Equation (3b) can be rewritten in:

$$\dot{C} = -\alpha C + \beta, \tag{12}$$

where

$$\alpha = \frac{k_d\tau(\sigma I)^2}{1 + \tau\sigma I} + k_r,\ \beta = \frac{k_d\tau(\sigma I)^2}{1 + \tau\sigma I}. \tag{13}$$

The evolution of C deduced from Equation (12) in light phase ($t \in [t_{2i}, t_{2i+1}]$) can be expressed by:

$$C(t) = \frac{\beta}{\alpha}\left(1 - e^{-\alpha(t-t_{2i})}\right) + C(t_{2i})e^{-\alpha(t-t_{2i})}, \tag{14}$$

where

$$C(t_{2i}) = \frac{\beta}{\alpha} \cdot \frac{(1 - e^{-\alpha T\varepsilon})}{e^{k_r T(1-\varepsilon)} - e^{-\alpha T\varepsilon}}. \tag{15}$$

The average value of C during light phase ($t \in [t_{2i}, t_{2i+1}]$) (noted as $\bar{C}_L$) is:

$$\begin{aligned} \bar{C}_L &= \frac{1}{T\varepsilon} \cdot \int_{t_{2i}}^{t_{2i+1}} C(t)\, dt, \\ &= \frac{\beta}{\alpha} + \left(\frac{\beta}{\alpha^2 T\varepsilon} - \frac{C(t_{2i})}{\alpha T\varepsilon}\right) \cdot \left(e^{-\alpha T\varepsilon} - 1\right). \end{aligned} \tag{16}$$

The growth rate in the light phase (noted as μ_L) is deduced from Equation (4) and Equation (11):

$$\mu_L = \gamma(1 - C), \tag{17}$$

where

$$\gamma = \frac{k\sigma I}{1 + \tau\sigma I}. \tag{18}$$

In periodic regime, the average gross growth rate in light phase ($t \in [t_{2i}, t_{2i+1}]$) (light period integrated, noted as $\bar{\mu}_L$) can then be obtained:

$$\bar{\mu}_L(I) = \frac{1}{T\varepsilon} \cdot \int_{t_{2i}}^{t_{2i+1}} \gamma(1 - C)\, dt = \gamma(1 - \bar{C}_L). \tag{19}$$

where $\bar{C}_L$ is given by Equation (16).

2.3 Respiration variation

In this model, we assume that respiration (noted as R) varies in light and dark phases, following a dynamics described in Equation (20):

$$\dot{R} = k_R(\chi_R(I) - R), \tag{20}$$

where k_R is the evolution rate (s^{-1}) of the respiration rate (s^{-1}), and

$$\chi_R(I) = \begin{cases} R_L, if I > I_{min}, \\ R_D, if I \leq I_{min}, \end{cases} \tag{21}$$

R_L and R_D are two constants, representing the highest respiration rate in light (R_L, s^{-1}), and the lowest respiration rate relieved in dark phase (R_D, s^{-1}), respectively. We assume that the actinic light I_{min} is much lower than the values of I experimented during the light phases. Since in periodic regime $R(t_{2i-1}) = R(t_{2i+1})$, the cycle time average respiration $\bar{R}$ is deduced by integrating Equation (20):

$$\begin{aligned} \frac{1}{T}\int_{t_{2i-1}}^{t_{2i+1}} \dot{R}\, dt = 0 = \frac{k_R}{T}\Big(\int_{t_{2i-1}}^{t_{2i}} R_L\, dt + \int_{t_{2i}}^{t_{2i+1}} R_D\, dt\Big) \\ - \frac{k_R}{T}\int_{t_{2i-1}}^{t_{2i+1}} R\, dt \\ \bar{R} = \frac{1}{T}\int_{t_{2i-1}}^{t_{2i+1}} R\, dt = R_L\varepsilon + R_D(1 - \varepsilon) \end{aligned} \tag{22}$$

2.4 The net growth rate in biofilm

In a square-wave L/D cycle, the cycle time average photosynthetic growth rate (called the gross growth rate in the following) is $\bar{\mu}_L(I) \cdot \varepsilon$.

When the light penetrates the biofilm, its intensity is attenuated following the Lambert-Beer law, meaning that, at each depth z the light intensity is

$$I(z) = I_0 e^{-k_z z}. \tag{23}$$

where k_z is the light extinction coefficient. Note that $k_z = \frac{1}{z}\ln\frac{I_0}{I(z)}$. The Beer Lambert equation can be rewritten as $dI = -k_z I dz$. The net growth rate (photosynthetic minus respiration) (noted as $\bar{\bar{\mu}}(I_0)$) of the film averaged over time is obtained by the integration of the local growth, as obtained by the local light intensity, along the film depth:

$$\begin{aligned} \bar{\bar{\mu}}(I_0) &= \frac{1}{h}\int_0^h \bar{\mu}_L(I(z))\varepsilon\, dz - \bar{R} \\ &= \frac{1}{\ln\frac{I_0}{I(h)}}\int_{I(h)}^{I_0} \frac{\bar{\mu}_L(I)\varepsilon}{I} dI - \bar{R}. \end{aligned} \tag{24}$$

3. MODEL RECALIBRATION AND VALIDATION

We aim at determining a vector of model parameter $p = (k, k_r, k_d, \tau, \sigma, R_L)$ that minimizes the error between the simulated state vector μ_{sim} and the measured state vector μ_m. For this purpose, the likelihood function of the error has to be maximized with respect to p. Assuming that the error is distributed according to a Gaussian white noise with a diagonal covariance matrix, this is equivalent to minimize the optimization criterion $\Psi_{MLE}(p)$:

$$\Psi_{MLE}(p) = \sum_{k=1}^{K}\sum_{j=1}^{J}\left(\frac{\mu_{m_{k_j}} - \mu_{sim_{k_j}}}{\sigma_k}\right)^2, \tag{25}$$

Where σ_k is the standard deviation of measured growth rates of each light regimes. K is the total number of light regimes tested, and J is the number of the replicates of each tested light regime. k and j are the order of light regimes and replicates, respectively. The Matlab Nelder-Mead simplex direct search minimization algorithm (*fminsearch*) was used and initialized with the first parameter guess (Han model parameters values from (Wu and Merchuk, 2001) respiration rate from (Grenier et al., 2019)), as shown in Table 1.

The net specific growth rate is computed from the experimental light transmittance as the slope of the regression between $ln(ln\frac{light\ input}{light\ output})$ and time t. Different light regimes were used to recalibrate the model. Continuous light with intensities of 100, 200, 310, 500 $\mu\text{mol} \cdot \text{m}^{-2} \cdot \text{s}^{-1}$ were considered. D/L represents the dark phase duration/light phase duration. Four intermittent light regimes with peak light intensity of 310 $\mu\text{mol} \cdot \text{m}^{-2} \cdot \text{s}^{-1}$ (D/L = 10s/5s; 60s/30s; 2min/1min), 500 $\mu\text{mol} \cdot \text{m}^{-2} \cdot \text{s}^{-1}$ (D/L = 20s/5s) were also used in the recalibration procedure. The model was validated with two intermittent light regimes with peak light intensity of 310 $\mu\text{mol} \cdot \text{m}^{-2} \cdot \text{s}^{-1}$(D/L = 8s/4s) and 400 $\mu\text{mol} \cdot \text{m}^{-2} \cdot \text{s}^{-1}$(D/L = 5s/5s). The validated parameter values are shown in Table 1, except the value of R_D which is set at $9.15 \cdot 10^{-8}$ s^{-1}.

Table 1. Validated biological parameters of Han model and respiration rate for biofilm growth rate simulation

Parameters	First guess	Calibrated value	Unit
k	$8.70 \cdot 10^{-6}$	$4.90 \cdot 10^{-6}$	$\text{s} \cdot \text{s}^{-1}$
k_r	$6.80 \cdot 10^{-3}$	$1.16 \cdot 10^{-2}$	s^{-1}
k_d	$2.99 \cdot 10^{-4}$	0.15	/
σ	$4.70 \cdot 10^{-2}$	$1.59 \cdot 10^{-2}$	$\mu\text{mol}^{-1} \cdot \text{m}^2$
τ	0.25	$1.06 \cdot 10^{-3}$	s
R_L	$1.5 \cdot 10^{-6}$	$1.78 \cdot 10^{-6}$	s^{-1}

4. RESULTS

4.1 Cycle time effect

Fig. 2A displays the net growth rate dynamic response to cycle times of the intermittent light regimes. With the same average light intensity, the shorter cycle time leads to higher growth rate compared to longer time scale. This is in agreement with the work of (Hartmann et al., 2014). For cycle time larger than 15 min light integration is no more observed, and the maximum level of photoinhibition is induced, as presented in Fig. 2C. In the range of seconds to tens of seconds, an intermediate regime is reached, which is not represented in (Hartmann et al., 2014). *Full light integration* is obtained for cycle time shorter than 100 ms. In these conditions, the inhibition rate decreases to the same level of the one for the equivalent constant average light (see Fig. 2C). In the end, a higher growth rate with flashing light is obtained due to the lower average respiration rate than the one triggered by constant light.

Fig. 3 shows the evolution of the inhibited state with respect to the light regimes. With continuous illumination, the inhibition level remains constant with time, and it increases with increasing light intensity. Interestingly, even a limiting light intensity of 100 $\mu\text{mol} \cdot \text{m}^{-2} \cdot \text{s}^{-1}$ presents an inhibition level of 25%. With intermittent light regimes, the C proportion follows a periodic pattern: decreasing in the dark phase due to the reparation of the damaged

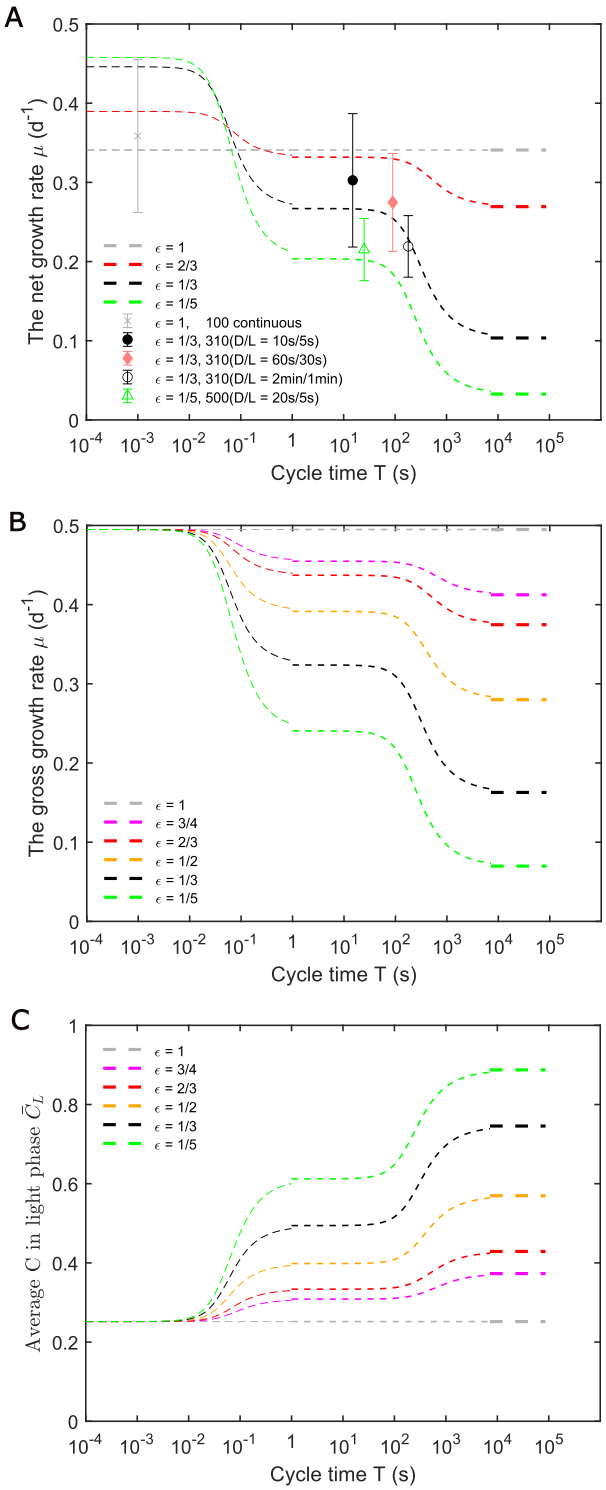

Fig. 2. Cycle time effect on biofilm net growth rate (A), on biofilm gross growth rate (B), and the average C in light phase $\bar{C}_L$ (C) with different light fractions. The average light intensity is set at 100 $\mu\text{mol} \cdot \text{m}^{-2} \cdot \text{s}^{-1}$. (A) shows the experimental outputs (mean and standard deviation) fitting with model predictions.

D1 proteins and increasing in the light phase. Compared to light regimes with the same duty cycle of 1/3 (310 μmol $\cdot$ m$^{-2}\cdot$s^{-1} (D/L = 10s/5s; 60s/30s; 2min/1min), light regime with cycle time of 3 min induces higher maximum inhibition level than 90 s and 15 s. As only the C proportion in the light phase matters for growth, the average C in the light phase with different duty cycles is presented in Fig. 2C. This explains the response of growth rate to different light regimes in Fig. 2B.

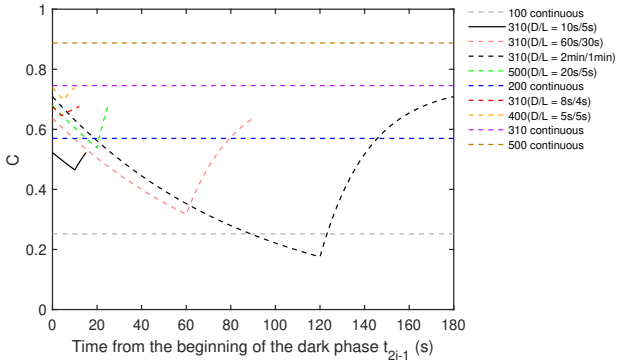

Fig. 3. C evolution in one photoperiod for each light regime studied

4.2 Light fraction effect

Light fraction effect on the net growth rate is presented in Fig. 4A for the various light regimes studied. With cycle time from 15 s to 3 min, the growth rate is positively impacted by the light fraction. As cycle times of 15 s and 25 s are the second plateau range (Fig. 2), the improvement of growth rate under 310 μmol $\cdot$ m$^{-2}\cdot$s^{-1} (D/L = 10s/5s) compared with that at 500 μmol $\cdot$ m$^{-2}\cdot$s^{-1} (D/L = 20s/5s) is due to effect of light fraction. The underlying reason is presented in Fig. 4B. With different cycle time scales ($T > 1$ ms), average C in the light phase decreases with light fraction, thus leading to a higher growth rate (see Fig. 4A). The inhibition level at different cycle time magnitudes are more significant when the light fraction is close to 0, which means intense but short light peaks. By contrast, a light fraction close to 1 indicates that the light regime is close to the continuous light regime with the same average light intensity. It is worth noting that there is not much difference in inhibition level between the different light regimes with larger light fractions. Especially, C remains the same at different duty cycles when cycle time is 1 ms, corresponding to the *full light integration* plateau in Fig. 2B and Fig. 2C.

5. DISCUSSION

The proposed model, improving Han's model (Han., 2001) by including respiration dynamics, reproduces the experimental biofilm growth behavior at different cycle time scales and light fractions. On the contrary to the existing models (Takache et al., 2015), this model can simulate the non-linear partial light integration with short cycle time orders and give important leads for growth rate optimization. The point is that we computed the average growth rates in any regime as a function of the light/dark

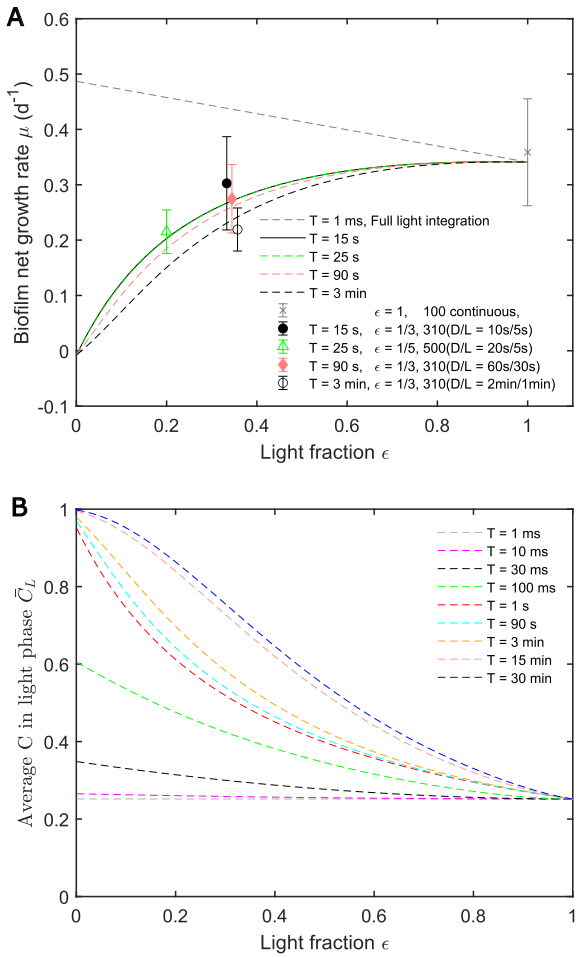

Fig. 4. With the same average light intensity of 100 μmol $\cdot$ m$^{-2}\cdot$s^{-1}: (A), growth rate with respect to light fraction. Growth rate of fluctuating light regimes are fitted in the figures and compared with constant light regimes. Light regimes 310 μmol $\cdot$ m$^{-2}\cdot$s^{-1} (D/L = 10s/5s; 60s/30s; 2min/1min) share the same light fraction: 1/3, but the latter two light regimes are shifted slightly on the right side to better distinguish from each other. Experimental data are shown with mean and standard deviation. (B), The average C in light phase with respect to light fraction at different cycle time scales.

signal. This made the model calibration straightforward, since it was not necessary to integrate slow-fast differential equations on very long time scale, making minimization procedures more efficient. The model fits well with observations with a p value of $0.0093 < 0.05$.

The photosynthetic efficiency computation, and the associated inhibition level, were so far determined only for duty cycles $\varepsilon = 0.5$ (Hartmann et al., 2014). The cycle time effect on biofilm growth rate presented in Fig. 2 is consistent with the observations of (Toninelli et al., 2016). Fig. 2B shows that *full light integration* phenomenon occurs in tens of milliseconds scale, in agreement with the study of (Vejrazka, 2012). From our model, this time order is the same for different light fractions. The difference between the net growth rate obtained for light/dark regimes and continuous light (ε of 1, grey line) is only 3 % with ε

of 2/3 (red line) for T around 100 s. This is invisible from experimental data, which will be considered in both cases as *full light integration*. But the difference is more significant with smaller ε at the same time magnitude. This is coherent with the work of (Toninelli et al., 2016) where*full light integration* was observed at cycle time of seconds with the light fraction of 0.5, but was not detected with the light fraction of 0.33 even cycle time shortened down to sub-seconds citepToninelli2016.

No light integration is predicted at tens of minutes, which is supported by (Grenier et al., 2019) focusing in *Chlorella autotrophica* biofilms . Interestingly, this time order seems longer than that published (seconds or hundreds of seconds) for planktonic cultures (Xue et al., 2011; Graham et al., 2017). More importantly, the characteristic inflexion point (second plateau in Fig. 2) occurs in different cycle time orders compared with planktonic *Chlamydomonas reinhardtii* cultures at 10-20 ms (Vejrazka, 2012).

6. CONCLUSION AND PERSPECTIVES

Light/dark regimes have been broadly studied in the literature to identify light regimes which optimize microalgae growth. So far, the analytical computation of the solutions of the Han model were not available for duty cycles different from 0.5 or 1. Considering light induced respiration phenomenon deeply affects the model outcomes, and it seems that this feature is specific to photosynthetic biofilms. The model is still sketchy, and further work would be necessary to better understand the respiration dynamics in response to fluctuating light.

REFERENCES

Bara, O., Bonnefond, H., and Bernard, O. (2019). Model development and light effect on a rotating algal biofilm. *IFAC-PapersOnLine*, 52(1), 376–381.

Beardall, J., Burger-Wiersma, T., Rijkeboer, M., Sukenik, A., Lemoalle, J., Dubinsky, Z., and Fontvielle, D. (1994). Studies on enhanced post-illumination respiration in microalgae. *Journal of Plankton Research*, 16(10), 1401–1410.

Bhattacharya, M. and Goswami, S. (2020). Microalgae–a green multi-product biorefinery for future industrial prospects. *Biocatalysis and Agricultural Biotechnology*, 25, 101580.

Costa, J.A.V., Freitas, B.C.B., Santos, T.D., Mitchell, B.G., and Morais, M.G. (2019). Open pond systems for microalgal culture. In *Biofuels from Algae*, 199–223. Elsevier.

Graham, P.J., Nguyen, B., Burdyny, T., and Sinton, D. (2017). A penalty on photosynthetic growth in fluctuating light. *Scientific reports*, 7(1), 1–11.

Grenier, J., Bonnefond, H., Lopes, F., and Bernard, O. (2019). The impact of light supply to moving photosynthetic biofilms. *Algal Research*, 44, 101674.

Gross, M., Mascarenhas, V., and Wen, Z. (2015). Evaluating algal growth performance and water use efficiency of pilot-scale revolving algal biofilm (rab) culture systems. *Biotechnology and bioengineering*, 112(10), 2040–2050.

Han., B.P. (2001). Photosynthesis-irradiance response at physiological level: A mechanistic model. *Journal of theoretical biology*, 213(2), 121–127.

Han, B.P. (2002). A mechanistic model of algal photoinhibition induced by photodamage to photosystem-ii. *Journal of theoretical biology*, 214(4), 519–527.

Hartmann, P., Béchet, Q., and Bernard, O. (2014). The effect of photosynthesis time scales on microalgae productivity. *Bioprocess and biosystems engineering*, 37(1), 17–25.

Huang, Y., Xiong, W., Liao, Q., Fu, Q., Xia, A., Zhu, X., and Sun, Y. (2016). Comparison of chlorella vulgaris biomass productivity cultivated in biofilm and suspension from the aspect of light transmission and microalgae affinity to carbon dioxide. *Bioresource technology*, 222, 367–373.

Mantzorou, A. and Ververidis, F. (2019). Microalgal biofilms: A further step over current microalgal cultivation techniques. *Science of the Total Environment*, 651, 3187–3201.

Martín-Girela, I., Curt, M.D., and Fernández, J. (2017). Flashing light effects on co2 absorption by microalgae grown on a biofilm photobioreactor. *Algal research*, 25, 421–430.

Mata, T.M., Martins, A.A., and Caetano, N.S. (2010). Microalgae for biodiesel production and other applications: a review. *Renewable and sustainable energy reviews*, 14(1), 217–232.

Megard, R., Tonkyn, D., and Senft, W. (1984). Kinetics of oxygenic photosynthesis in planktonic algae. *Journal of Plankton Research*, 6(2), 325–337.

Milledge, J.J. and Heaven, S. (2013). A review of the harvesting of micro-algae for biofuel production. *Reviews in Environmental Science and Bio/Technology*, 12(2), 165–178.

Sforza, E., Simionato, D., Giacometti, G.M., Bertucco, A., and Morosinotto, T. (2012). Adjusted light and dark cycles can optimize photosynthetic efficiency in algae growing in photobioreactors. *PloS one*, 7(6), e38975.

Takache, H., Pruvost, J., and Marec, H. (2015). Investigation of light/dark cycles effects on the photosynthetic growth of chlamydomonas reinhardtii in conditions representative of photobioreactor cultivation. *Algal Research*, 8, 192–204.

Toninelli, A.E., Junfeng Liu, M., Wu, H., and Liu, T. (2016). Scenedesmus dimorphus biofilm: Photoefficiency and biomass production under intermittent lighting. *Scientific Reports*, 6, 1–10. doi:10.1038/srep32305.

Vejrazka, C. (2012). *Microalgal photosynthesis under flashing light*. Wageningen University and Research.

Wang, J., Liu, W., and Liu, T. (2017). Biofilm based attached cultivation technology for microalgal biorefineries-a review. *Bioresource Technology*, 244. doi: 10.1016/j.biortech.2017.05.136.

Wu, X. and Merchuk, J.C. (2001). A model integrating fluid dynamics in photosynthesis and photoinhibition processes. *Chemical engineering science*, 56(11), 3527–3538.

Xue, S., Su, Z., and Cong, W. (2011). Growth of spirulina platensis enhanced under intermittent illumination. *Journal of biotechnology*, 151(3), 271–277.